

Coupling Difficulty Associated with Interchain Clustering and Phase Transition in Solid Phase Peptide Synthesis

James P. Tam* and Yi-An Lu

Contribution from the Department of Microbiology and Immunology, Vanderbilt University, Nashville, Tennessee 37232-2363

Received August 4, 1995[⊗]

Abstract: We have developed a model containing clustered peptide chains to evaluate coupling difficulties associated with interchain interactions in solid phase peptide synthesis. Our results revealed two new findings. First, there was a significant difference in solvation properties between the conventional dispersed and our clustered peptide chain models at a similar level of peptidyl loading. At the completion of an eight-residue peptide, with a peptide content of >61%, the solvated volumes of a dispersed chain model increased 20–30-fold over the initial dry resin and were about 4–5-fold higher than those of the clustered chain model in both polar and nonpolar solvents. The decrease in solvation mimics the effect of higher cross-linking of resin supports, leading to poor swelling ability. Second, there was a polystyrene to polyamide transition when the peptide loading reached approximately 50% of the peptidyl resin. In this transition phase, the swelling and growth of the peptidyl resin reached the lowest point in both polar aprotic and hydrophobic solvents. Furthermore, the phase transition was also the crossover point where the aprotic polar solvent *N,N*-dimethylformamide provided better resin swellability than the nonpolar solvent dichloromethane. A good correlation between swelling ability and the coupling yield in aprotic polar solvents was also found. A combination of the aprotic polar solvent NMP and coupling at elevated temperature was found to be the most efficient to increase coupling efficiency. Thus, our results provide evidence for coupling difficulties associated with the interchain interactions exacerbated by chain clustering and phase transition.

Introduction

High efficiency of chain assembly in solid phase peptide synthesis is an essential component of the scheme.¹ Recent studies have shown that an average stepwise yield of 99.93% can be achieved under optimized conditions with the conventional, copoly(styrene–1% divinylbenzene) resin.² Such a high repetitive yield in coupling reactions to the growing peptide chains is an important contributing factor to the successful synthesis of several long and complex peptides.^{3–6} Despite these successes, difficulties in chain assembly have been reported and often cited as a leading source of frustration for the assembly of large peptides.^{7,8}

A leading cause of coupling difficulties has become partially clarified and appears to be steric occlusion of peptide chains within the polymeric network. The steric effect is contributed by the interplay of several factors including (i) peptide sequence, (ii) sterically hindered amino acids, and (iii) hydrogen bonding

contributed by the peptide–polymeric backbone,⁹ intrachain,^{2,10,11} or interchain interactions.^{7,8,12–14} Of these factors, contributions by hydrogen bonding are probably the most severe, which often result in poor solvent or reagent permeability accompanied by sudden shrinkage or insufficient swelling of the peptidyl resin networks.

Among the three types of hydrogen bonding interactions, contribution due to peptide–polymeric backbone has been found to be small because coupling difficulty is independent of the nature of the resin support currently available commercially.¹⁵ Often a similar amino acid sequence will encounter coupling difficulty with the Merrifield type of polystyrene or the Sheppard type pendant polyamide resin.¹⁶ Coupling difficulty due to intrachain or interchain hydrogen bonding is frequently sequence dependent. Intrachain interactions occur most frequently at reverse turns^{10,11} whereas interchain interactions occur when ordered structures such as helices or β -sheets are formed within peptidyl resins, creating a network of interchain hydrogen bonding, which leads to desolvation, steric hindrance to coupling

* To whom correspondence should be addressed at the Department of Microbiology and Immunology, Vanderbilt University, A5119 MCN, 1161 21st Ave. S., Nashville, TN 37232-2363. Phone: (615) 343-1465. Fax: (615) 343-1467.

[⊗] Abstract published in *Advance ACS Abstracts*, December 1, 1995.

(1) Merrifield, R. B. *J. Am. Chem. Soc.* **1963**, *85*, 2149–2154.

(2) Merrifield, R. B.; Singer, J.; Chait, B. *Anal. Biochem.* **1988**, *174*, 399–414.

(3) Tam, J. P. *Int. J. Pept. Protein Res.* **1987**, *29*, 421–43.

(4) Nutt, R. F.; Brady, S. F.; Darke, P. L.; Ciccarone, T. M.; Colton, C. D.; Nutt, E. M.; Rodkey, J. A.; Bennett, L. H.; Waxman, C. D.; Sigal, I. S.; Andweson, P. S.; Veber, D. F. *Proc. Natl. Acad. Sci. U.S.A.* **1988**, *85*, 7129–7133.

(5) Gras-Masse, H.; Ameisen, J. C.; Boutillon, C.; Gesquiere, J. C.; Vian, S.; Neyrinck, J. L.; Drobeq, H.; Capron, A.; Tartar, A. *Int. J. Pept. Protein Res.* **1990**, *36*, 219–226.

(6) Clarke-Lewis, I.; Aebersold, R.; Zittener, H.; Schrader, J. W.; Hood, L. E.; Kent, S. B. H. *Science* **1986**, *231*, 134–9.

(7) Kent, S. B. H. *Peptide: Structure and Function*, Proceedings of the Ninth American Peptide Symposium; Deber, C. M., Ed.; Pierce Chemical Co.: Rockford, IL, 1985; pp 407–414.

(8) Kent, S. B. H. *Annu. Rev. Biochem.* **1988**, *57*, 959–989.

(9) Sheppard, R. C. In *Innovation and Perspectives in Solid Phase Synthesis. Peptides, Polypeptides and Oligonucleotides*; Epton, R., Ed.; Intercept Ltd.: Andover, England, 1992; pp 213–219.

(10) Live, D. H.; Kent, S. B. H. In *Peptides: Structure and Function*; Hruby, V. J., Rich, D. H., Eds.; Pierce Chemical Co.: Rockford, IL, 1983; pp 65–68.

(11) Merrifield, R. B. *Makromol. Chem. Macromol. Symp.* **1988**, *19*, 31–67.

(12) Mutter, M.; Vuilleumier, S. *Angew. Chem., Int. Ed. Engl.* **1989**, *28*, 535–554.

(13) Milton, R. C. d. L.; Milton, S. C. F.; Adams, P. A. *J. Am. Chem. Soc.* **1990**, *112*, 6039–6046.

(14) Deber, C. M.; Lutek, M. K.; Heimer, E. P.; Felix, A. M. *Pept. Res.* **1989**, *2*, 184–188.

(15) Kent, S. B. H.; Alewood, D.; Alewood, P.; Baca, M.; Jones, A.; Schnolzer, M. In *Innovation and Perspectives in Solid Phase Synthesis. Peptides, Polypeptides and Oligonucleotides*; Epton, R., Ed.; Intercept Ltd.: Andover, England, 1992; pp 1–22.

(16) Hoeprich, P. D., Jr. In *Innovation and Perspectives in Solid Phase Synthesis. Peptides, Polypeptides and Oligonucleotides*; Epton, R., Ed.; Intercept Ltd.: Andover, England, 1992; pp 49–55.

reagents, and poor accessibility to the α -amino group of peptide chains. Predictive methods¹³ for interchain interactions have been attempted, but correlation of the secondary structure of protected peptides on a resin support in organic solvents is unreliable, and often structures found in aqueous solution differ from those in their protected forms in organic solvents when attached to resin supports. An example is decaalanine, a known α -helix in solution, which has been shown to encounter severe coupling difficulty during its solid phase synthesis² attributed to intrachain hydrogen bonding, but recent measurements by IR¹⁷ show that it may exist as interchain β -sheets. Nevertheless, a common cause of most coupling difficulty can be attributed to interchain interactions.

Coupling difficulties due to interchain interactions are particularly well documented in solution synthesis where solubilities of peptides decrease with the increase of peptide lengths.^{18,19} Similarly, in solid phase peptide synthesis, interchain interaction is known to be dependent on the density of peptide chains.^{20,21} A high density of peptide chains may produce poor swelling in solvents because they mimic a higher degree of cross-linking that results in less swellability. Thus, resin with a high level of substitution will likely produce a higher frequency of coupling difficulties.²⁰ However, poor couplings have been frequently observed in those resins with a moderate level of substitutions. A contributing factor could be the way resins are manufactured. Nearly all functionalized polystyrene resins from commercial sources are postderivatized by the Friedel-Crafts reactions on unfunctionalized polystyrene beads to give chloromethyl, aminomethyl, and benzyldiamino moieties.²²⁻²⁴ The use of a strong acid catalysis coupled with the large-scale reaction could render uneven derivatization highly probable. This leads us to propose that coupling difficulty may be attributed to interchain interaction when the functional sites on the resins are unevenly distributed, leading to chain clustering that mimics cross-linking and limits resin swellability as well as reagent permeability.

Another well-documented phenomenon in coupling difficulty is the occurrence of interchain interactions in the initial stage of the synthesis between residues 5 and 15 where 3-4 consecutive residues encountered coupling difficulties which disappear after this junction of synthesis.^{7,8} An explanation for this general phenomenon is that the peptides acquire the propensity to form secondary structure, particularly β -sheet formation. We, however, offer an additional explanation. We propose that such interchain interaction is exacerbated by chain clustering at the phase transition when the peptide content reaches nearly 50% of the polystyrene, becoming predominantly a polyamide resin. Thus, when resins are not functionalized evenly, local clusters of high-density peptide chains are created at an environment of the phase transition that favors interchain interactions among the growing peptide chains.

To substantiate this hypothesis, we employ a model that produces chain clustering to exacerbate interchain interactions

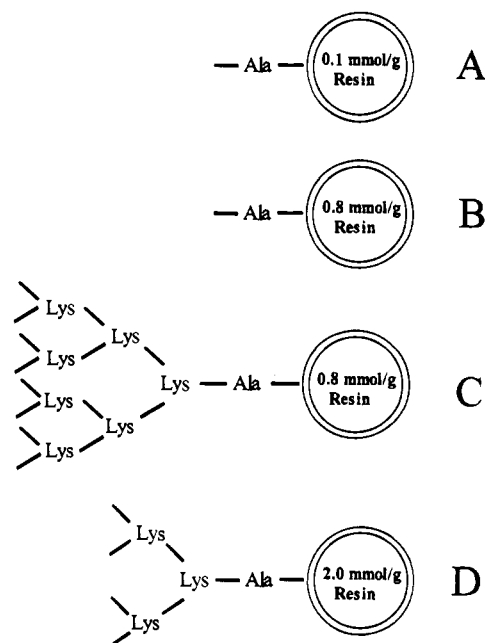


Figure 1. Four models representing dispersed peptide chains (models A and B) and clustered peptide chains (models C and D) on the resin support.

in the resin. This is achieved with a model containing branched peptides with a cascade arrangement, commonly known as multiple antigen peptides (MAP) for immunological uses.^{25,26} These cascade branched peptides are synthesized on the resin support with a core matrix containing several levels of branched lysines for the attachment of eight dendritic peptide chains. Thus, this model system amplifies peptide chains in the resin support 8-fold to form a cluster that allows us to evaluate the effect of interchain interactions. Recently we have found difficulty in the synthesis of the peptide sequence Phe-Gln-Tyr-His-Ser-Lys-Glu-Gly (FG-8). This sequence contains three aromatic residues and five benzyl-protecting groups [Phe-Gln-Tyr(BrZ)-His(Dnp)-Ser(Bzl)-Lys-(ClZ)-Glu(OBzl)-Gly] and favors interchain β -sheet formation. For comparison, we also prepared FG-8 on resins with dispersed peptide chains conventionally used in peptide synthesis. In this paper, we describe the use of the clustered and dispersed peptide chain models and the protected form of the sequence of FG-8 to evaluate coupling difficulties associated with interchain interactions and phase transition.

Results

Branched Oligomeric Matrix To Amplify Interchain Interactions. To evaluate interchain interactions, we synthesized four peptide models consisting of different peptide:polymer ratios as well as the geometric distribution of peptide chains on copoly(styrene-1% divinylbenzene) resins (Figure 1). The first model was a dispersed low-loading peptide chain at a 0.1 mmol/g substitution (designated model A). It contained uniformly dispersed peptide chains in the resin support conventionally used in solid phase peptide synthesis. The second model was a moderate-loading peptide chain at a 0.8 mmol/g substitution (designated model B). It also contained uniformly dispersed peptide chains. This level of substitution is popular and routinely used for peptide synthesis. The third model was derivatized from model A with an octameric matrix consisting of three levels of branched lysines to produce a clustered and

(17) Larsen, B. D.; Christensen, D. H.; Holm, A.; Zillmer, R.; Nielsen, O. F. *J. Am. Chem. Soc.* **1993**, *115*, 6247-6253.

(18) Narita, M.; Doi, M.; Sugawara, H.; Ishikawa, K. *Bull. Chem. Soc. Jpn.* **1985**, *58*, 1473-1479.

(19) Narita, M.; Ogura, T.; Sato, K.; Honda, S. *Bull. Chem. Soc. Jpn.* **1986**, *59*, 2433-2438.

(20) Sarin, V. K.; Kent, S. B. H.; Mitchell, A. R.; Merrifield, R. B. *J. Am. Chem. Soc.* **1984**, *106*, 7845-7850.

(21) Kent, S. B. H.; Merrifield, R. B. In *Peptide 1980*; Brunfeld, K., Ed.; Scriptor: Copenhagen, 1981; pp 328-333.

(22) Feinberg, R. S.; Merrifield, R. B. *Tetrahedron* **1972**, *28*, 5865-5871.

(23) Mitchell, A. R.; Erickson, B. W.; Ryabtser, M. N.; Hodges, R. S.; Merrifield, R. B. *J. Am. Chem. Soc.* **1976**, *98*, 7357-7361.

(24) Pietta, P. G.; Marshall, G. R. *J. Chem. Soc. D.* **1970**, 650-651.

(25) Tam, J. P. *Proc. Natl. Acad. Sci. U.S.A.* **1988**, *85*, 5409-5413.

(26) Tam, J. P.; Lu, Y. A. *Proc. Natl. Acad. Sci. U.S.A.* **1989**, *86*, 9084-9088.

Table 1. Volume Ratio of Peptides of Dispersed Low-Loading Model A, Dispersed Moderate-Loading Model B, and Clustered Peptide Model C

solvent	model	volume ratio ^a at various peptide/resin loadings (%)								
		5	10	15	20	30	40	50	60	70
DCM	A	1.98	2.43	2.78	2.79					
	B		9.06	6.90	6.27	5.26	3.86	4.42	4.53	3.92
	C	1.98	1.80	1.81	1.81	2.06	1.82	1.72	1.78	1.75
DMF	A	2.00	1.83	2.07	2.63					
	B		5.40	4.50	4.55	3.78	3.66	3.95	4.88	4.50
	C	2.00	1.84	1.98	2.09	2.30	2.50	2.56	2.73	2.64
NMP	A	2.45	2.45	2.81	2.91					
	B		8.33	6.35	5.91	4.93	3.93	4.33	5.39	5.59
	C	2.45	2.79	2.84	3.01	3.02	2.57	2.99	3.13	3.39
DMSO	A	1.41	1.98	2.31	2.72					
	B		4.13	4.55	5.01	4.70	4.05	4.51	5.13	5.07
	C	1.41	1.42	1.84	2.01	2.06	1.76	2.10	2.10	2.04

^a Volume ratio = swelling volume/dry resin in a specific synthetic cycle.

branched peptide model with a loading of 0.8 mmol/g substitution (designated model C) and an 8-fold amplification from model A. It also contained a similar loading of peptides as model B but with a geometric distribution based on the cascade-branched peptide design introduced by our laboratory.^{25,26} The fourth model, a high-loading clustered peptide chain model (designated model D), contained a high substitution at 2 mmol/g which was formed by derivatizing model B using a four-branched matrix consisting of three lysines. This model was designed specifically to examine the coupling yield of superhigh peptide loading. An extension of Lys-Lys-Ala at the C-terminus was used in the dispersed model to compensate for the branched structures of the clustered models C and D.

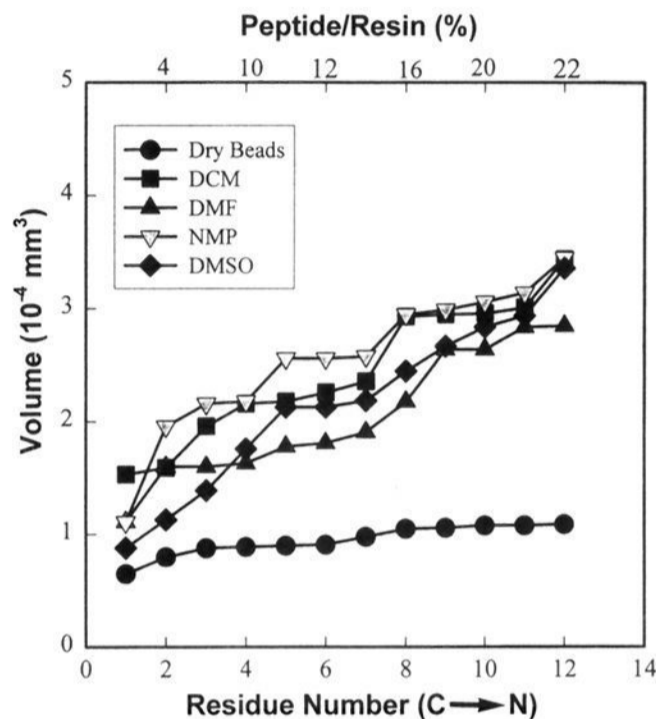
Models A–D with an octapeptide, FG-8 (FQYHSKEG), sequence were synthesized by Boc chemistry. At the completion of the synthesis, the peptide content of models A–C reached 22, 61, and 72%, respectively. The difference of the peptide content in models B and C is due to weight correction of the octameric lysine core matrix. An additional 11 residues [PNVCRMATDIL where C = Cys(Acm)] were assembled on the high-loading clustered model D at the end of the synthesis of model sequence FG-8 to determine the effect of chain length on coupling efficiency.

Resin Volume in Different Solvents. To determine the effect of interchain interactions in the dispersed and clustered models, solvation volumes of the peptidyl resins at the completion of each synthetic cycle were measured in solvents including dichloromethane (DCM), *N,N*-dimethylformamide (DMF), *N*-methylpyrrolidinone (NMP) and dimethyl sulfoxide (DMSO), and their combinations which are often used for optimizing dissolution of amino acid derivatives were used in the determination of solvent effects. Peptidyl resin volumes were determined by directly measuring the diameters under a light microscope. Beads (100–200 mesh) preswollen in solvent were spread over a grid-lined hemacytometer with a cover glass to minimize solvent evaporation. A total of about 800 beads for each determination were sampled in triplicate to obtain an average diameter. In general, solvent-swollen beads with good swelling properties such as those in models A and B exhibited a round, smooth, and translucent appearance while the corresponding beads with poor swelling properties such as those in models C and D were rugged and less translucent with dark patches. The solvation effect was defined by the volume ratio (VR) which measured the ratio of the swollen and the dry resin in a given solvent and in a specific synthetic cycle. Furthermore, we used the growth ratio (GR) to define the ratio of solvated

Table 2. Growth Ratio of Peptides of Dispersed Model B and Branched Clustered Model C at Similar Peptide/Resin Loadings

solvent	model	growth ratio ^a at various peptide/resin loadings (%)							
		10	15	20	30	40	50	60	70
DCM	B	9.06	9.20	9.33	9.47	11.31	13.25	18.70	19.84
	C	2.46	2.48	2.51	2.89	3.20	3.37	3.54	3.63
DMF	B	5.51	5.91	6.17	6.81	10.75	11.89	20.17	25.87
	C	2.52	2.71	2.89	3.22	4.38	4.92	5.40	5.47
NMP	B	8.30	8.33	8.67	8.87	11.54	12.99	22.26	30.06
	C	3.82	3.89	4.17	4.18	5.02	5.89	6.17	7.04
DMSO	B	4.15	4.94	7.01	8.49	11.89	13.50	21.21	29.91
	C	1.94	2.52	2.78	2.89	3.09	3.74	4.15	4.25

^a Growth ratio = swollen resin/dry resin at a given cycle at the beginning of the synthesis.

**Figure 2.** Measured bead size of the dispersed chain of model A at 0.1 mmol/g substitution in different solvents.

volume at a given synthetic cycle and the initial volume of dry resin at the beginning of the synthesis.

The VR at each synthetic cycle (Table 1) provided useful insights into the influence of solvents as the peptide content increases on the peptidyl resin. The GR (Table 2) provided an overall assessment for the solvation effect on the peptidyl resin.

A model A which has a dispersed low-loading peptide chain, the GR grew 4.06–4.55-fold in all solvents or solvent combinations (Figure 2) at 22% of the final peptide content on polystyrene resin. The VRs showed a steady increase during the chain assembly in all solvents. DCM as well as NMP provided higher solvent swellability than DMF and DMSO or solvent combinations such as NMP–DMSO and DMF–DMSO (Figure 2 and supporting information). However, the differences in the swelling properties among these solvents are small since the initial amino acid substitution on this resin was low, and the peptidyl resin at the completion of the synthesis retained the polystyrene characteristics.

In the moderate-loading models B and C which have an 8-fold higher peptide content than model A, there were significant differences in both the magnitudes and profiles of their solvation in polar and nonpolar solvents (Figures 3 and 4 and supporting information). These differences are summarized in Figures 5 and 6. The dispersed-chain model exhibited a dynamic range of responses to solvation of polar and nonpolar solvents as the peptide content progressed from a polystyrene to a polyamide, while the clustered-chain model was largely unresponsive with a small linear increase in both VRs and GRs (Tables 1 and 2).

With a final peptide loading of 71% on the resin at the completion of the synthesis, the final GRs of the dispersed-

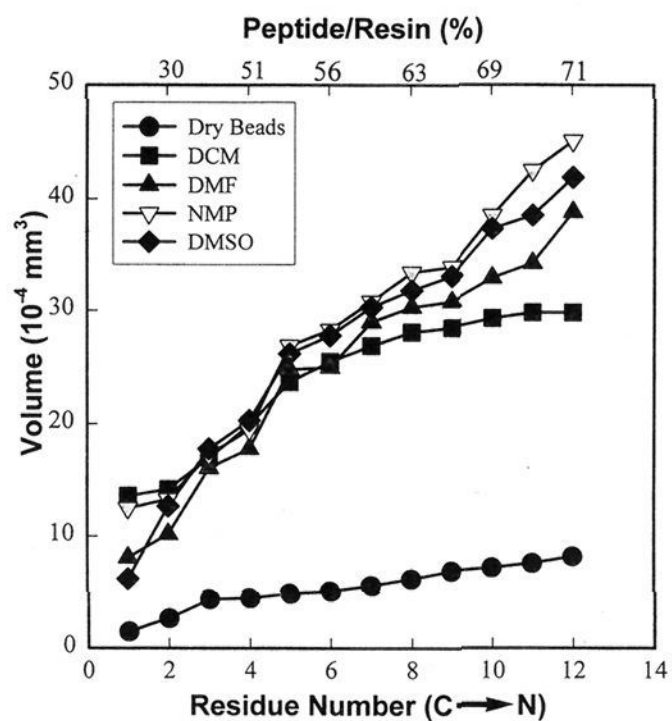


Figure 3. Measured bead size of the dispersed chain of model B at 0.8 mmol/g substitution in different solvents.

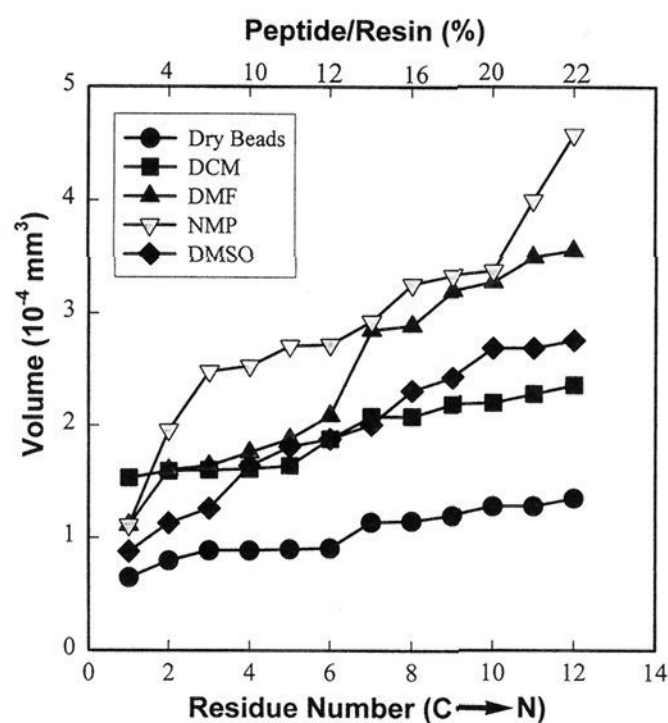


Figure 4. Measured bead size of the clustered chain of model C at 0.8 mmol/g substitution.

chain model B grew 25–30-fold in polar and nonpolar solvents (Table 2) while the GRs of clustered-chain model C reached 3.6 in DCM and 5.5–7 in polar solvents such as DMF, DMSO, or NMP. The difference between the dispersed- and clustered-chain models was about 4–5-fold. Solvent combinations containing 10% aprotic polar solvents such as DMF, NMP, or DMSO did not influence the VRs or GRs. In general, NMP appears to be the best swelling solvent for all three models (Figures 2–4).

The polymeric phase transition and a broad transition point as the peptide vs styrene content approaches the ratio of 1:1 (w/w) are clearly visible in Figures 5 and 6. This transition was evident only in the dispersed-chain model. This point marked the difference in solvation behavior between polar and nonpolar solvents where the peptide/resin became more of a polyamide and solvated better in aprotic polar solvents. The GR reached the lowest point but increased rapidly after the peptide content reached 50%. The GR showed a dramatic increase after the transition point in all solvents. For example,

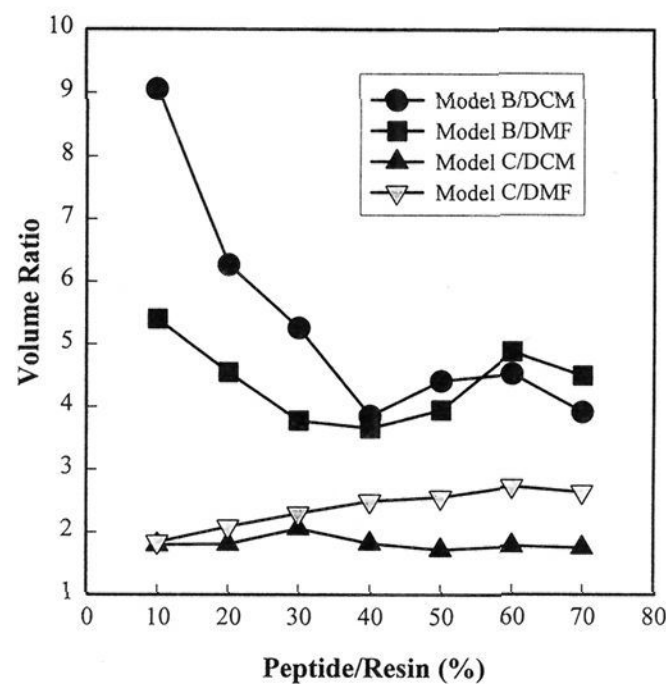


Figure 5. Comparison of volume ratio (solvated/dried volume at each synthetic cycle) of model B (dispersed) vs model C (clustered peptide chains).

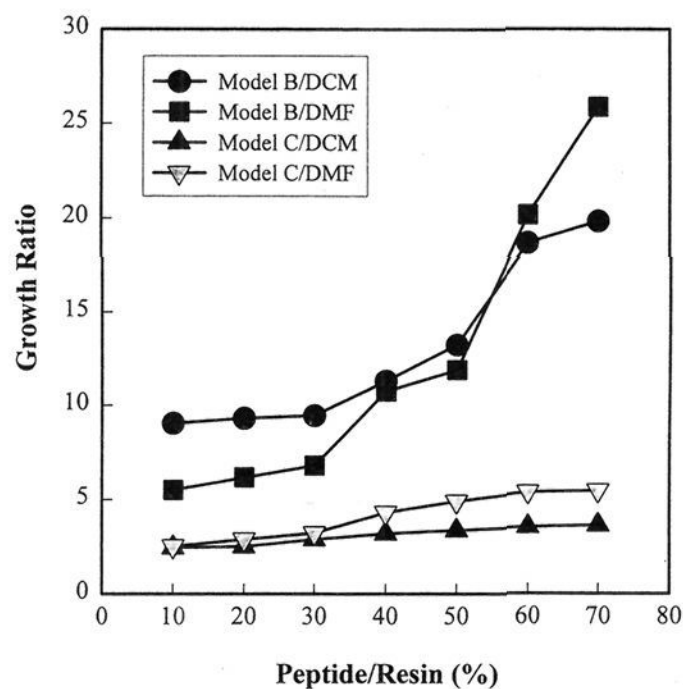


Figure 6. Comparison of growth ratio (solvated volume at a specific cycle/dried volume) of model B (dispersed) vs model C (clustered peptide chains).

the GR of model B in DMF was 10.75 at 40%, 11.89 at 50%, and 20.17 at 60% peptide content (Figure 5). Similar observations were found in NMP and DMSO.

Coupling Yields. Coupling yields were measured by the quantitative ninhydrin method,²⁷ and the popular coupling protocols^{1,28,29} including 1,3-dicyclohexylcarbodiimide (DCC) (Figure 7), DCC/HOBt (1-hydroxybenzotriazole), and (benzotriazol-1-yloxy)tris(dimethylamino)phosphonium hexafluorophosphate (BOP) (supporting information) were studied. In the dispersed models A and B, with substitutions of 0.1 and 0.8 mmol/g, respectively, all couplings proceeded smoothly irrespective of the coupling methods (Figure 7). Each coupling yield averaged >99.41%. In the clustered model C, coupling yields of the first three lysines were similar to those of models A and B. However, except for one residue (Gly), after the octabranched matrix was completed, difficulties in coupling were encountered in the seven other residues, especially in residues 5–8 which averaged about 95% (Figure 7). These results showed that DCC/DCM was a good coupling method for the conventional peptide model, but was not a suitable method for the clustered model. Improvements were observed

(27) Sarin, V. K.; Kent, S. B. H.; Tam, J. P.; Merrifield, R. B. *Anal. Biochem.* **1981**, *117*, 147–151.

(28) Coste, J.; Le-Nguyen, D.; Castro, B. *Tetrahedron Lett.* **1990**, *31*, 205–208.

(29) Knorr, R.; Trzeciak, A.; Bannworth, W.; Gillessen, D. *Tetrahedron Lett.* **1989**, *30*, 1927–1930.

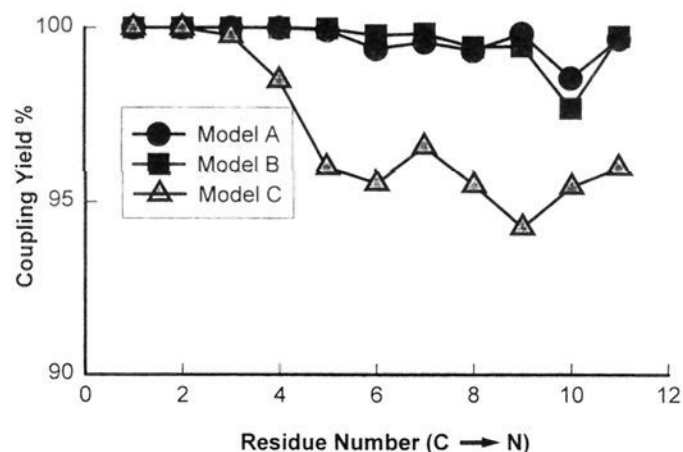


Figure 7. Comparison of coupling yields in DCC/DCM of dispersed peptide models A and B and clustered peptide model C. The sequence from C to N is AKKKGEKSHYQF.

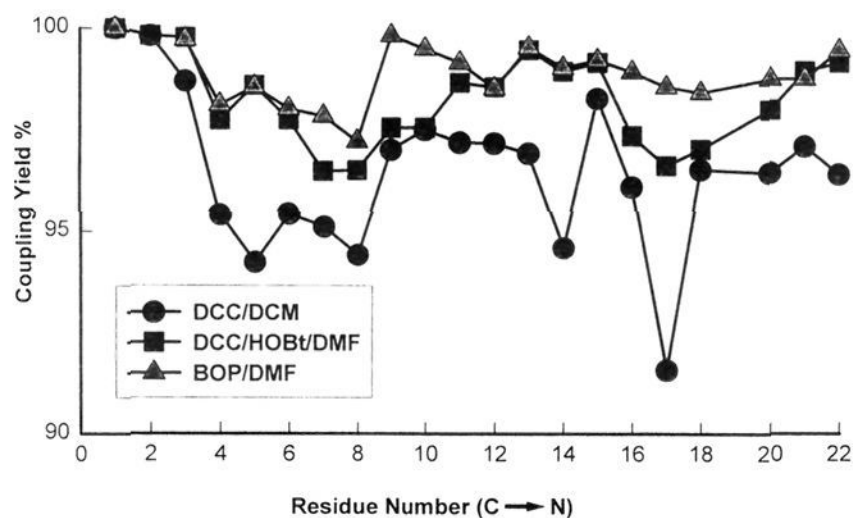


Figure 8. Comparison of coupling yields of the highly clustered peptide model D in different coupling protocols. The sequence from C to N is AKKKGEKSHYQFLIDTAMRC(Acm)VNP.

using the aprotic polar solvent-based coupling reagents including DCC/HOBt/DMF, DCC/HOBt/NMP, and DCC/HOBt/NMP–DMSO (9:1 v/v) (supporting information) as well as BOP in DMF and NMP (supporting information). Coupling yields improved to 97.11–98.04% in DMF and to 98–99.75% in NMP and NMP–DMSO combination solvents. These results are consistent with previous findings^{15–19} that sequence-dependent coupling difficulties could be partially improved by the use of aprotic polar solvent combinations.^{7–14} Significant improvement was, however, achieved under elevated temperature to 50 °C for 30 min (supporting information) to reach 99.13–99.79%. An elevated coupling temperature increases the entropy and diminishes interchain interaction. Both factors enhance complete coupling. With a very high density of peptide chains on the resin support, such as in model D, a satisfactory coupling yield of the FG-8 sequence (residues 5–12, Figure 8) was difficult to achieve even in an aprotic polar solvent.

Model D also illustrates the “sequence-dependent” coupling difficulty as well as the interchain interaction exacerbated by chain clustering and phase transition. Although couplings in the FG-8 sequence encountered little difficulty in the dispersed-chain models A and B, they were significantly poorer in high-density clustered-chain model D, particularly after the trilyl branched point from residues 5–8 (C → N direction). The average coupling yield was 95% in DCM and 97% in DMF for these four residues as compared to 99.4% in DCM and DMF found in models A or B. In model D, the coupling yield in DMF improved after residue 8 and averaged 98.5% for the next 14 residues even though the peptidyl resin became predominantly a polyamide. Similarly, the coupling in DCM improved to about 96.7% after residue 8 but largely remained at this level for residues 9–22 (C → N direction).

Discussion

This paper describes two new findings that correlate with coupling difficulties in solid phase peptide synthesis. The first involves interchain peptide interactions that limit the swelling of peptidyl resin and solvent permeability. Our results using a clustered and branched peptide model provide direct evidence for the occurrence of interchain interactions when clusters of peptide chains are formed in the resin. The effect of interchain interaction exacerbated by the chain clustering is very pronounced and simulates cross-linking both physically and morphologically (data not shown). In a branched peptide resin with moderate loading (of 0.8 mmol/g) such as model C, the clustered effect renders only 4- and 5.5-fold growth in DCM and DMF, respectively, when the peptide content reaches 61% of the resin content. In contrast, model B with dispersed peptide chains at a similar level of substitution grows nearly 20- and 26-fold in DCM and DMF, respectively. The swelling properties of the clustered model C are so poor that they are similar to those of the dispersed model A containing only 0.1 mmol/g substitution and 22% peptide content.

The second finding involves the polystyrene to polyamide phase transition and is best illustrated by Figures 5 and 6. Before the transition point, the solvation power of DCM is greater than that of DMF or DMSO. The polystyrene character diminishes as the peptide weight increases and becomes more of a polyamide. With our particular peptide sequence, the transition point is broad and occurs at 30–50% of peptide to polystyrene (w/w). After the transition point, the solvation power of DCM (a polystyrene-like solvent) becomes less than that of DMF (a polyamide-like solvent). The transition point is also where both solvents are the least effective and the peptide resins the least swellable (Figure 5). This type of broad transition is sequence dependent and may account for the initial stage of coupling difficulties between 5 and 15 residues often observed in peptide synthesis.^{7,8} An effective solvent that allows the coupling reagent to freely permeate the solvent-swollen peptide–polymer matrix will likely enhance the coupling efficiency. Our results show that there is a strong correlation between solvent permeability and coupling yields and NMP is the solvent of choice to overcome interchain interaction and to improve coupling efficiency.

Our results also confirm the previous finding by Sarin et al.²⁷ regarding the dynamic and growing properties of the swollen peptidyl resin networks during the peptide chain assembly. They have found that the peptidyl resin with an 80% peptide content containing a linearly repeating tetrapeptide–oxyphenylacetyl unit produces GRs of 12 and 28 in DCM and DMF, respectively. Our dispersed peptide chain model B with a 71% peptide loading gives GRs of 20 and 26, respectively, in DCM and DMF. The GRs of this model in DMF are comparable to those obtained by Sarin et al. However, there is a difference in the GR in DCM which could be attributed to the nature of the resin, the peptide sequence, and protecting groups being used. Nevertheless, these results show that the peptidyl resin network is not static and has no predetermined limit of space available for the peptide chain within the network.

Two general strategies are available for overcoming coupling difficulties, due to interchain interaction in the synthesis of nonbranched peptides. The first strategy uses physical means including the use of elevated temperature,³⁰ solvent mixtures

(30) Tam, J. P. In *Peptides: Structure and Function*; Deber, C. M., Hruby, V. J., Kopple, K. D., Eds.; Pierce Chemical Co.: Rockford, IL: 1985; pp 423–425.

(31) Yamashino, D.; Blake, J.; Li, C. H. *Tetrahedron Lett.* **1976**, *18*, 1469–1472.

containing trifluoroethanol,³¹ and denaturants or chaotropic agents.^{32,33} The second strategy uses chemical means involving the replacement of the secondary amide bond by a reversible tertiary bond, thus eliminating the amide hydrogen that forms the interchain hydrogen bonding network. Two types of reversible amide bond protecting groups have been developed. The approach by Johnson et al.³⁴ uses the 2-hydroxy-4-methoxybenzyl (Hmb) group which is cleavable by TFA. The Hmb group is an improvement toward the ease of the amino acylation with the incoming amino acid of the hindered dimethoxybenzyl group developed by Narita et al.³⁵ and proposed by Blackmeer et al.³⁶ at suitable intervals, usually 6–8 residues apart to break up interchain interaction. Pseudo-oxaproline has also been proposed by Mutter et al.³⁷ to form an oxazolidine ring of the Ser/Thr residues.³⁷ Reversible protecting groups of this type, such as thioproline, have also been developed by Rich and Tam³⁸ and Kemp³⁹ but have not been applied to this problem.

Apart from coupling difficulty caused by β -seet tendency, implications derived from our results point to the quality of resin supports. First, the use of a low-loading resin is advantageous for the synthesis of branched peptides to minimize interchain interactions. Second, poorly prepared resins often result in poor solvation properties and lead to horrendous synthesis with deletion products. A likely cause is that these resins are rich in clustered functional sites. Finally, to prevent site clustering, resin prepared from polymerization of prederivatized monomers may hold potential promise.

Experimental Procedures

Materials. Boc-Ala-OCH₂-Pam resin (0.8 mmol/g) was purchased from Applied Biosystems (Foster City, CA), and the 0.1 mmol/g resin was prepared according to Mitchell et al.²⁹ DMF, NMP, and DCM were purchased from Baxter without purification. DMSO and DIEA were purchased from Aldrich. BOP and HBTU were from Richelieu Biotechnologies (Canada). Boc-amino acid was obtained from Bachem, Inc. (Torrance, CA). The following side chain protecting groups were used in synthesis: Glu(OBzl), His(Dnp), Lys(CIZ), Ser(Bzl), Tyr(BrZ), Arg(Tos), Asp(OBzl), Cys(Acm), and Thr(Bzl). The microscope was from Olympus IMT-2.

Measurement of Bead Size. Diameters of the unswollen and dry peptidyl resin beads (100–200 mesh) were measured directly under the light microscope. Representative samples were obtained by the following procedure. After each of the synthetic cycles and determination of the coupling yield by the ninhydrin test,²⁷ the resins were washed with DMF and DCM. The resins (200–300 beads) were withdrawn with silanized glass tubes containing different solvents. The dried beads were kept at room temperature overnight in a vacuum. Other samples were swollen overnight in solvent. A sample of dry beads was spread over the gridline of a hemacytometer with a cover glass to prevent the evaporation of solvent, the diameters of each of

200–300 beads were measured, and the average diameter was obtained by averaging the sample number. For accuracy the microscope was focused at the outer edge of each bead. Measurements of swelling beads were performed with use of the same process. The bead sizes were calculated by averaging the diameters of all resin beads by using the formula $1/6\pi d^3$.

Coupling Protocols. (a) In Situ 1,3-Dicyclohexylcarbodiimide (DCC) Coupling (DCC/DCM). The standard solid phase DCC method was used. The Boc-amino acid (4 equiv relative to the amino component) in dichloromethane (DCM) was added to the reaction vessel, followed by DCC (4 equiv) in DCM. The activation and coupling were continued for 1 h. The peptide resin was filtered and washed with *N,N*-dimethylformamide (DMF) and DCM.

(b) In Situ 1-Hydroxybenzotriazole (HOBt) Coupling (DCC/HOBt/DMF). The Boc-amino acid (4 equiv) in DMF was added to the reaction vessel. HOBt (4 equiv) and DCC (4 equiv) in DCM were then introduced separately to the reaction. The coupling continued for 1.5 h. A similar protocol was used for NMP, DMF:DMSO = 9:1 (v/v), NMP:DMSO = 9:1 (v/v).

(c) Preformed Symmetric Anhydride Coupling in *N,N*-Dimethylformamide (PSA/DMF). The Boc-amino acid (4 equiv) was dissolved in DCM. DCC (2 equiv) in DCM was added, and after activation for 10 min, the resulting anhydride solution was transferred to a round-bottom flask with filtration. After DCM was evaporated, the anhydride was redissolved in DMF and then added to the reaction vessel. The coupling continued for 30 min.

(d) BOP Coupling in Dichloromethane (BOP/DCM). The Boc-amino acid (3 equiv) in DCM was added to the reaction vessel. BOP reagent (3 equiv) in DCM and *N,N*-diisopropylethylamine (6 equiv) were then added. The coupling continued for 45 min. The same protocol was used for BOP/DMF and HBTU/DMF coupling.

(e) Elevated Coupling Temperature. The Boc-amino acid (4 equiv) in DMF was added to the reaction vessel with a heating water jacket. DCC (4 equiv) in DMF and HOBt (4 equiv) in DMF were introduced. The coupling continued for 30 min at 50 °C. The resin was filtered and washed with DMF and DCM. After each single coupling, about 5 mg of resin was withdrawn with a tube. The resin was dried overnight in a vacuum. Quantitative results were obtained in the ninhydrin monitoring reaction.²⁷

Synthesis of the Core Matrix. The core matrices of octabranched and tetrabranched peptides were synthesized as described previously.^{25,26} The synthesis of the first level of the carrier core to form Boc-Lys-(Boc)-Ala-OCH₂-Pam resin was achieved using a 4-fold excess of Boc-Lys(Boc) DCHA via (benzotriazol-1-yloxy)tris(dimethylamino)phosphonium hexafluorophosphate (BOP) in dichloromethane. The second and third levels were synthesized by the same protocol to give the octabranched Boc-Lys-(Boc) core matrix.

Acknowledgment. This work was funded by NIH Grants CA36544 and AI35577.

Supporting Information Available: Figures showing the measured bead size of the dispersed chain of model A at 0.1 mmol/g substitution and the clustered chain of model C at 0.8 mmol/g substitution in different solvents and comparisons of coupling yields of the moderately clustered peptide model C in DCC/HOBt coupling protocols (the sequence from C to N is AKKKGEKSNYQF), in BOP coupling protocols, and at elevated temperature (5 pages). This material is contained in many libraries on microfiche, immediately follows this article in the microfilm version of the journal, can be ordered from the ACS, and can be downloaded from the Internet; see any current masthead page for ordering information and Internet access instructions.

JA952630K

(32) Hain, K. W.; Klis, W. A.; Stewart, J. M. *Science* **1990**, *248*, 1544–1547.

(33) Pugh, K. C.; York, E. H.; Stewart, J. M. *Int. J. Pept. Protein Res.* **1992**, *40*, 208–213.

(34) Johnson, T.; Quibell, M.; Owen, D.; Sheppard, R. C. *J. Chem. Soc., Chem. Commun.* **1993**, 369–372.

(35) Narita, M.; Fukunaga, T.; Wakabayashi, A.; Ishikawa, K.; Nakano, H. *Int. J. Pept. Protein Res.* **1984**, *23*, 306–314.

(36) Blaakmeer, J.; Tijssse-Klasen, T.; Tesser, G. I. *Int. J. Pept. Protein Res.* **1991**, *37*, 556–564.

(37) Haack, T.; Mutter, M. *Tetrahedron Lett.* **1992**, *33*, 1589–1592.

(38) Rich, D. H.; Tam, J. P. *Tetrahedron Lett.* **1977**, *9*, 749–750.

(39) Kemp, D. S. *Biopolymers* **1981**, *20*, 1793–1804.